PHYSICAL REVIEW B **67**, 121402(R) (2003)

Steering effect on the shape of islands for homoepitaxial growth of Cu on Cu(001)

Jikeun Seo,[1] S.-M. Kwon,[2] H.-Y. Kim,[2] and J.-S. Kim[2]
[1]*Division of General Education, Chodang University, Muan 534-701, Republic of Korea*
[2]*Department of Physics, Sook-Myung Women's University, Seoul 140-742, Republic of Korea*
(Received 28 October 2002; revised manuscript received 21 January 2003; published 10 March 2003)

The steering effect on the growth of islands is investigated by combining molecular dynamics (MD) and kinetic Monte Carlo (KMC) simulations. Dynamics of incident atoms and kinetics of atoms on a substrate are realized by MD and KMC, respectively. The reported experimental results on the asymmetric island growth [van Dijken *et al.*, Phys. Rev. Lett. **82**, 4038 (1999)] is well reproduced. A salient phenomenon, the reversal of the asymmetry, is found as the island size increases and attributed to the asymmetric flux on the lower terrace of islands.

DOI: 10.1103/PhysRevB.67.121402 PACS number(s): 68.35.−p, 68.37.−d

The growth of thin film is an essential step for many modern technologies and scientific investigation, and a lot of efforts have been made to understand and tailor the growth process. There have been many studies on the effect of energetic[1] and kinetic[2] variables to the growth of thin film, while minor attention has been paid to the role of dynamic variables such as deposition conditions. Recently, van Dijken, Jorritsma, and Poelsema[3] report the growth of rectangular Cu islands on square-symmetric Cu(001) when the deposition is made at grazing incidence. Furthermore, they control the shape of Co island on Cu(001) by varying the deposition angle and successfully manipulate its magnetic anisotropy.[4] Their work clearly reveals the importance of dynamic variable and expands the adjustable parameters for the growth of thin film.

An atomistic picture for the asymmetric island growth is also proposed by van Dijken, Jorritsma, and Poelsema.[3] Incident atoms see a modified potential by preexisting islands and as a result the incoming flux is focused on the upper terrace of the islands near the front edge, while depleted on the lower terrace near the rear edge of the islands. Such steering effect is argued to result in the shortened edge length along the deposition direction, *x*-axis, and leaves the edge perpendicular to the deposition direction, *y*-axis, relatively longer. The model, however, is based on a qualitative argument without any detailed kinetic description on island growth from the inhomogeneous flux distribution, and the steering effect is considered only in the incident plane rather than in the three dimensional space as it should be. Independently, Zhong *et al.*[5] propose that the enhanced corner crossing diffusion of the incident atoms at the front edge due to the transient mobility or their enlarged kinetic energies by the attraction of the atoms at the substrate, increases the growth speed along the *y*-direction relative to that along the *x* direction. However, the very existence and the role of the transient mobility still remains controversial.[6] Steering effect has also been studied for thin-film growth[7–9] by MD and nonlinear stochastic equations.[10] For the growth of a crystalline film, only recently Montalenti and Voter[11] report the steering induced instability of Ag film on Ag(001), but the study is restricted to the roughening of the film on a substrate near 0 K and to the deposition at normal incidence.

The purpose of the present study is to investigate the steering effect on the growth of asymmetric islands by performing a realistic simulation combining KMC and MD simulations; MD simulation is executed to calculate the trajectory of depositing atoms in *three*-dimensional space, when a deposition event is selected in KMC. Before the next deposition event is selected, various diffusion events of adatoms are realized by KMC simulation.[12] In the present study, the asymmetric island shape observed in the experimental study[3] is well reproduced. Moreover, a salient phenomenon, the reversal of the asymmetry of island from elongation in the *y* direction to that in the *x* direction, is found as the coverage or the substrate temperature increases. The asymmetric shape of the island is attributed mainly to the asymmetric deposition flux on the lower terrace of island that in turn depends on its size.

For the deposition events, Lennard-Jones(LJ) potential in the form of $U(r)=4D[(\sigma/r)^{12}-(\sigma/r)^{6}]$ with $D=0.4093$ eV and $\sigma=2.338$ Å is used for the interaction between the incident atom and surface atoms,[6] and Verlet algorithm is adapted. The simulation box is composed of 6 layer high empty space in *z* direction on an fcc(001) surface of 400 $\times$400 lattice with periodic boundary condition in the xy plane. (The surface lattice constant, $a_0=2.56$ Å and the interlayer spacing, $d=1.805$ Å.) The incident atom starts at the initial height of $10a_0$ along [110] direction. The initial kinetic energy (0.15 eV) is determined from the melting temperature of Cu. The atom follows a trajectory determined from the interaction with preexisting atoms frozen on the substrate until it experiences the repulsive force, and thereat one deposition event ends. For the diffusion events, 11 different processes are taken into account including those suggested by Furman *et al.*[13] Some of the most influential diffusion barriers are listed in Table I.

The mound radius, which can directly be compared with the diffraction results,[3] is determined from the simulated morphology as the first zero of the height-height correlation function, $\langle h(\mathbf{r})h(0)\rangle-\langle h\rangle^2$. To increase the statistical reliability, simulations are performed 60 times under the same growth condition and the mound radius is calculated over the whole set of simulated morphologies.

In Fig. 1 we summarize the simulation results under the identical growth conditions to those of the previous experi-

TABLE I. Some of the diffusion barriers and diffusion parameters used in KMC. Notations in the bracket [ ] are from Furman *et al.* (Ref. 13).

Type of diffusion	Diffusion barrier
Single atom hopping $[E_0]$	0.485 eV
Dimer lateral bond break $[E_2]$	0.463 eV
Reestablishing NN bond $[E_4]$	0.183 eV
Erlich-Schwöbel (ES) barrier (ΔE_S)	0.1 eV
Jump frequency (ν_0t)	2.4×10^{13}
Deposition rate (F_0)	0.00416 ML/s

ment.[3] (We denote the mound radius along the x axis by L and that along the y axis by W.) For the normal deposition, W and L are identical at all coverages. When the deposition is made at 80° off the surface normal, however, the symmetry is broken and the difference between W and L becomes larger as the coverage increases. At 0.5 monolayer (ML), W is larger than L by 5% reproducing the previously reported result.[3] It is worth noting that the experimental result[3] could be reproduced without taking any transient mobility into account. The inset of Fig. 1 shows that for constant coverage of 0.5 ML, the aspect ratio, W/L, increases as a function of the deposition angle (from the surface normal). This result demonstrates that the asymmetry of the island shape is closely related to the reduced symmetry of the deposition geometry.

To analyze the effect of the reduced symmetry of the deposition process on the island growth, the two-dimensional distribution of the deposition flux is calculated at a deposition angle of 80°. The top figure in Fig. 2(a) reproduces the flux distribution along the x axis through the center of a preexisting island as reported in Ref. 3, which herein is called the front and rear edge (*FR-edge*) steering effect. A strong dependence of the flux distribution on the island size is additionally found in the present study as shown in Fig.

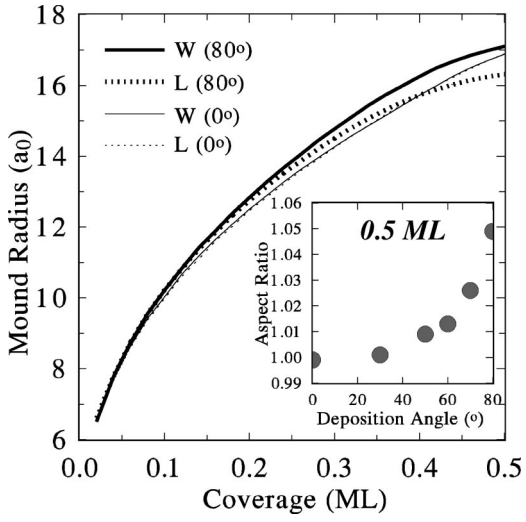

FIG. 1. Mound radius along both x and y directions for Cu islands grown on Cu(001) at 250 K as a function of the coverage. Inset: Aspect ratio of mound radii, W/L, versus deposition angle (from the surface normal).

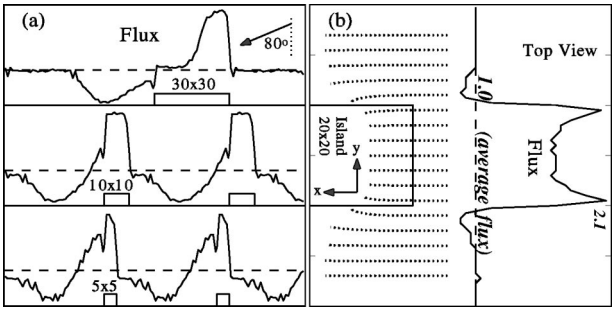

FIG. 2. The deposition flux and atomic trajectory calculated from MD simulation at deposition angle of 80°. (a) Deposition flux along the x axis through the center of a preexisting island of size, $30a_0$ (top), $10a_0$ (middle), and $5a_0$ (bottom), respectively. (b) Top view of the trajectory of incident atoms near a preexisting island and the flux distribution across the deposition direction. The flux is normalized to the average flux (long dashed line).

2(a); as the island size becomes smaller, the portion of the island with enhanced flux is enlarged. Besides, in Fig. 2(b), an unpredicted steering effect called herein the side edge (*S-edge*) steering is observed; the trajectories of incident atoms are curved toward both side edges and enhanced flux is found along both side edges. As will be discussed later, both the dependence of deposition flux on the island size and the relative strength of *FR-edge* steering to that of *S-edge* steering have great impact on shaping the island.

A series of simulation is performed with various substrate temperatures to investigate the kinetic effect in the asymmetric island growth. Figure 3 shows the dependence of L and W on the coverage at various growth temperatures. A stunning new phenomenon, the reversal of the asymmetry of island is found. At each temperature above 230 K, as the coverage increases a point (marked by + sign) is found, below which

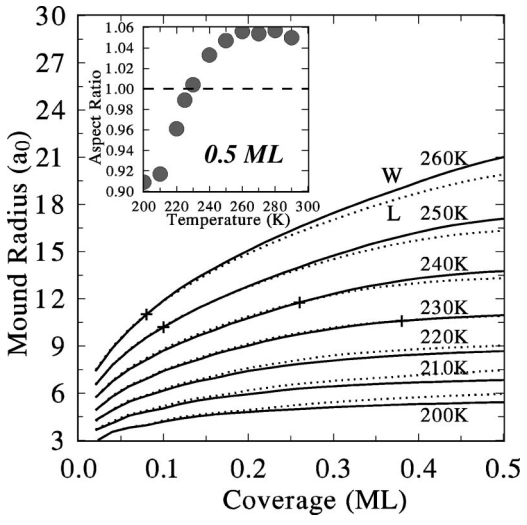

FIG. 3. Temperature and coverage dependence of mound radius. Solid curves represent mound radii (W) along y direction and dotted curves correspond to those (L) along x direction. + signs indicate the reversal points of the asymmetry. Inset: Temperature dependence of the aspect ratio (W/L) for 0.5 ML deposition.

$W<L$ and above which $W>L$. The inset summarizes the temperature dependence of the aspect ratio at 0.5 ML deposition; $W>L$ above 230 K as observed in Ref. 3, but $W<L$ below 230 K. Such reversal of the island shape has never been predicted before.

To understand such intricate temperature and coverage dependence of the asymmetric island growth, the effect of the inhomogeneous deposition flux on the island growth is explored in more detail. The inhomogeneous flux would manifest itself in two different ways; (1) asymmetric downhill current from the top of the island due to the asymmetric deposition flux on the island and (2) asymmetric deposition flux around the lower terrace of the island. As for the first one, the downhill current is estimated by counting the number of atoms coming over the *ES* barrier during the growth simulations. Despite the inhomogeneous deposition flux on the upper terrace of the island as shown in Fig. 2, the ratio of the downhill current per unit edge length over *x*-directional edges to that over *y*-directional edges is found to be very close to 1.0. This direction-independent or symmetric downhill current is due to the terrace diffusion on top of the island which is much more frequent than the downhill diffusion by $\sim 10^2$ times. As a result, the inhomogeneous deposition flux on the island is effectively homogenized before atoms come over *ES* barrier and hence it would not contribute to the asymmetric growth of island.

As for the second one, the distribution of the deposition flux on the lower terrace around the island is investigated. In Fig. 4(a), shown is the average deposition flux on lower terrace within $3a_0$ distance from the side edges (*S* terrace) and that from the front and rear edges (FR-terrace) as a function of the island size. Asymmetric distribution of the deposition flux can be clearly recognized over the whole range of island size. Furthermore, the flux on the FR-terrace decreases monotonically while that on the *S* terrace shows a maximum as the island becomes larger. For the island size smaller than $10a_0$, the flux on FR-terrace is larger than that on *S* terrace, but the reverse is true for the larger island.

The island-size dependence of the flux ratio as shown in Fig. 4(b) is quite similar to the temperature dependence of the aspect ratio of the islands as shown in the inset of Fig. 3. Keeping in mind that the mean island size monotonically increases with the substrate temperature for the same coverage, it suggests that the temperature dependence of the aspect ratio originates from the dependence of the flux ratio on the island size; At low substrate temperature where small islands form, the average flux on FR-terrace is larger than that on *S* terrace and results in asymmetric island having $L>W$, and *vice versa*.

This idea is examined further by plotting the aspect ratio of islands as a function of the mean size of islands formed with various substrate temperatures, diffusion parameters and deposition rates [Fig. 4(b)]. A strong correlation is found between the aspect ratio and the island size as expected, even though the data are collected from uncorrelated simulations. Furthermore, it reproduces all the features found in the dependence of the flux ratio on the island size, especially the crossover (aspect ratio=1). (The island sizes where the crossover in the aspect ratio occur are larger than the corresponding ones in the flux ratio. This is understood from the fact that the island size is determined by the integration of deposition flux.) It suggests that the most important factor determining the shape of the island is the flux distribution on the lower terrace of the island, which in turn is determined by the island size.

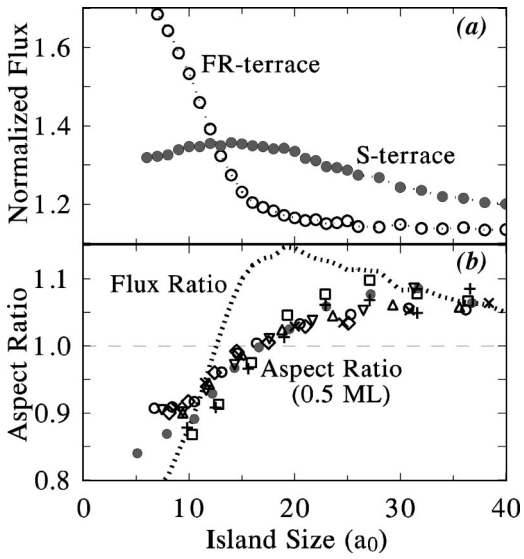

FIG. 4. Deposition flux and the aspect ratio according to the island size. (a) The filled and open circles represent the average deposition flux on *S*-terrace ($F_{\text{S-terrace}}$) and that on *FR*-terrace ($F_{\text{FR-terrace}}$), respectively. Each flux is normalized to the mean flux over the whole simulated area. (b) The ratio of deposition fluxes, ($F_{\text{S-terrace}}/F_{\text{FR-terrace}}$; dotted curve) and the aspect ratio (W/L) for 0.5 ML deposited with various temperatures (190 K–300 K) and diffusion parameters are plotted as a function of the island size: ○ (Table I), + ($\Delta E_{Sch}=0.05$ eV), □ ($\Delta E_{Sch}=0.00$ eV), ◇ ($\Delta E_{Sch}=0.15$ eV), ● ($E_2=0.553$ eV,$E_4=0.485$ eV), △ (deposition rate $1/2F_0$), × (deposition rate $1/12F_0$), ▽ ($\nu_0=1.2\times10^{13}$). The values in the parentheses are those varied from Table I.

If this conjecture is correct, the reversal of the asymmetry should also occur at similar island sizes regardless of the temperature or the coverage. The reversal of the asymmetry is indeed observed at similar island sizes, as indicated with + signs in Fig. 3, regardless of the substrate temperature, reassuring that the island-size dependence of the flux ratio at the lower terrace of the island is the critical factor for shaping the island.

Still it remains to find out the origin of such island-size dependence of the flux ratio. This could be understood from the flux distribution shown in Figs. 2 and 5. For small islands [Fig. 2(a) middle and bottom], the perturbed potentials at front and rear edges interfere and result in the increased flux on the FR-terrace. As the island size increases, the flux near the rear edge becomes relatively smaller [Fig. 2(a) top]. Hence, the *average* flux on the FR-terrace monotonically decreases as the island-size increases as found in Fig. 4(a).

On the other hand, the average flux on the *S* terrace is influenced by two counteracting factors; first, the flux on the *S* terrace increases with the island size, because the longer the edges the more atoms moving parallel to the side edges are attracted to the edges. However, the flux on *S* terrace is

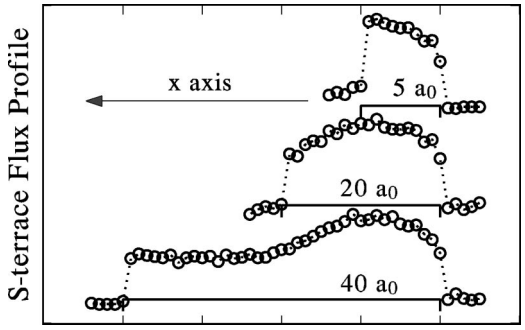

FIG. 5. Flux profile on *S* terrace along the side edge for islands of varying sizes, 5, 20, and 40 a_0 long. Each solid line represents both the position of a preexisting island and the average flux over the whole simulated area.

not homogeneous along the side edges due to a somewhat intricate variable involved (Fig. 5). For small islands (Fig. 5 top and middle), the deposition flux is enhanced over the whole edge. As the island-size increases, the relative portion of the side edge with pronounced flux enhancement gradually decreases (Fig. 5 bottom). This suggests that the *average* flux over the side edge will gradually decreases as the edge length increases. Hence, the competition between these two factors results in the maximum of the average flux at the island size of 17–20 a_0, explaining the dependence of the average flux on the island size as observed in Fig. 4(a). The origin of the inhomogeneous enhancement of flux along the side edge on *S* terrace can be found by comparing Fig. 5 with Fig. 2(a). The flux profile along the side edge (Fig. 5) shows quite a resemblance with that along the center line of the island in the deposition direction [Fig. 2(a)]. It suggests that the side edge flux is determined not solely by the *S-edge* steering but *cooperatively* by the *FR-edge* steering.

In summary, the present simulation combining MD and KMC properly reproduces the previously reported rectangular island growth of Cu/Cu(001) under deposition at a grazing incidence angle, and shows that the transient mobility is not a necessary condition for the asymmetric island growth. Instead, the asymmetry of the island shape is attributed mainly to the asymmetry of the deposition flux on the lower terrace of island. Also found is the reversal of the aspect ratio of asymmetric islands, which depends mainly on the island size. This, so far, unanticipated phenomenon remains to be proven by further experimental study. It is also found important that, for a proper interpretation of the experimental results, the steering effect should be treated in full three dimension.

S. V. Dijken is appreciated for many helpful comments. This work is supported by KOSEF(R06-2002-007-01002-0) and CSCMR. (JK)

[1] E. Bauer, in *The Chemical Physics of Solid Surfaces and Heterogeneous Catalysis*, edited by D. A. King and D. P. Woodruff (Elsevier, Amsterdam, 1984), Vol. 3B.

[2] H. Brune, Surf. Sci. Rep. **31**, 121 (1998); *The Chemical Physics of Solid Surfaces*, edited by D. A. King and D. P. Woodruff (Elsevier, Amsterdam, 1997), Vol. 8; *Morphological Organization in Expitaxial Growth and Removal*, edited by Z. Zhang and M. G. Lagally (World Scientific, Singapore, 1998).

[3] S.V. Dijken, L.C. Jorritsma, and B. Poelsema, Phys. Rev. Lett. **82**, 4038 (1999); S.V. Dijken, L.C. Jorritsma, and B. Poelsema, Phys. Rev. B **61**, 14 047 (2000).

[4] S. van Dijken, G.D. Santo, and B. Poelsema, Appl. Phys. Lett. **77**, 2030 (2000).

[5] J. Zhong, E. Wang, Q. Niu, and Z. Zhang, Phys. Rev. Lett. **84**, 3895 (2000).

[6] D.E. Sanders and A.E. DePristo, Surf. Sci. **254**, 341 (1991).

[7] W.D. Luedtke and U. Landman, Phys. Rev. B **40**, 11 733 (1989).

[8] D.E. Sanders, D.M. Halstead, and A.E. DePristo, J. Vac. Sci. Technol. A **10**, 1986 (1992).

[9] J. Yu and J.G. Amar, Phys. Rev. Lett. **89**, 286103 (2002).

[10] M. Raible, S.J. Linz, and P. Hänggi, Phys. Rev. E **62**, 1691 (2000).

[11] F. Montalenti and A.F. Voter, Phys. Rev. B **64**, R081401 (2001).

[12] Similar approach is found in the following article; S.W. Levine, J.R. Engstrom, and P. Clancy, Surf. Sci. **401**, 112 (1998).

[13] I. Furman, O. Biham, Jiang-Kai Zuo, A.K. Swan, and John F. Wendelken, Phys. Rev. B **62**, R10649 (2000).